Microelectronics Reliability 51 (2011) 30–37

Contents lists available at ScienceDirect

Microelectronics Reliability

journal homepage: www.elsevier.com/locate/microrel

Influence of gold pick up on the hardness of copper free air ball

J. Lee [a], M. Mayer [a,*], Y. Zhou [a], J.T. Moon [b], J. Persic [c]

[a] Microjoining Laboratory, Centre of Advanced Materials Joining, University of Waterloo, Waterloo, Canada N2L 3G1
[b] MK Electron Co. Ltd., Yongin, South Korea
[c] Microbonds Inc., Markham, Canada

ARTICLE INFO

Article history:
Received 21 July 2008
Received in revised form 22 March 2010
Accepted 22 March 2010
Available online 24 April 2010

ABSTRACT

The effect of substrate material pick up by the Cu wire tail on the hardness of the subsequently formed free air ball (FAB) is investigated with scanning electron microscopy (SEM) and micro-hardness test. The Cu wire bonds are made on Au metallization. Wire residue is not found on the imprint the tail bond leaves on the metallization, but fracture of the substrate metallization is evident. SEM images of the Cu wire tail end clearly show Au residue (pick up). The amount of Au pick up is estimated higher than 0.03% of the volume of a subsequently formed 50 μm diameter FAB, exceeding typical impurity and dopant concentrations (0.01%). Lowering the impact force process parameter is found to strongly increase the amount of substrate material pick up. Cu free air balls (50 μm in diameter) formed with an estimated Au pick up volume of 50 μm^3 are found to be between 1.2 HV and 4.3 HV softer than those without pick up. However, the hardness varies significantly more than that of FABs without pick up.

1. Introduction

Increasing demands for improved reliability, finer pitch interconnection [1] and cost reduction of IC packages encourage the use of Cu wire in the wire bonding process. The Cu wire to Al pad bonding system (Cu/Al bonds) can have four times longer life time than Au/Al bonds [2]. Thinner diameter Cu wire can be used to obtain the same electrical property compared to when thicker Au wire is used due to the lower electrical resistivity [3] and higher tensile strength and stiffness of Cu [4].

Chip damages such as pad peeling, cratering, or dielectric layer delamination have become major concerns in thermosonic Cu ball bonding processes [5–9]. As low-*k* materials which are mechanically weaker than SiO_2 are applied as dielectric layers in order to increase performance and decrease noise by cross talk in microelectronic devices, minimizing the chip damages becomes a challenge.

Previous studies report that the ultrasonic power [5] and bonding force [6] parameters have significant effects on chip damage during wire bonding. Oxide free and uniform Cu free air ball (FAB) formation is critical in the thermosonic Cu ball bonding process because oxidized FABs can cause defective bonds, bond lift off, and craters [10]. Harman [8] reported that the chip damage can occur sporadically in processes that otherwise produce reliable bonds. Onuki et al. [11] reported that high purity and annealing of FAB balls and shielding gas heating during electrical flame off (EFO) can reduce the hardness of the FAB.

Despite a number of studies performed [12–14], there is still lack of understanding of the sporadic occurrence of chip damage in thermosonic wire bonding. Especially, no studies have been reported on the possibility of metallization material been picked up by the wire tail during breaking from the metallization and the effect of such pick up on the Cu wire FAB formation and ball bonding process.

The present study provides evidence for substrate material (pick up) being present at the end of wire tail and gives more details on the effect of process parameters on the amount of pick up. The influence of the pick up material on the FAB hardness is quantified.

2. Definition of tail and wedge bonds

Tail breaking is part of not only the wedge bonding process but also the standard bond-off process used on each wire bonder to remove excess wire protruding from the capillary. Tail breaking produces a straight piece of wire with defined length (“tail”) protruding from the capillary suitable for subsequent FAB formation. The tail breaking force (TBF) was measured and optimized using a proximity sensor attached to the wire clamp [15]. The tail

Abbreviations: *BF*, bonding force; *BT*, bonding time; EFO, electrical flame off; FAB, free air ball; *ID*, impact type deformation; *IF*, impact force; PM1, process modification 1; PM2, process modification 2; PM3, process modification 2; *T*, bonding temperature; TBF, tail breaking force; *US*, ultrasonic power; UED, ultrasonic enhanced deformation; WCA, wire contact area; *WD*, width of WCA.

* Corresponding author.
E-mail addresses: j75lee@engmail.uwaterloo.ca (J. Lee), mmayer@uwaterloo.ca (M. Mayer).

0026-2714/$ - see front matter © 2010 Elsevier Ltd. All rights reserved.
doi:10.1016/j.microrel.2010.03.014

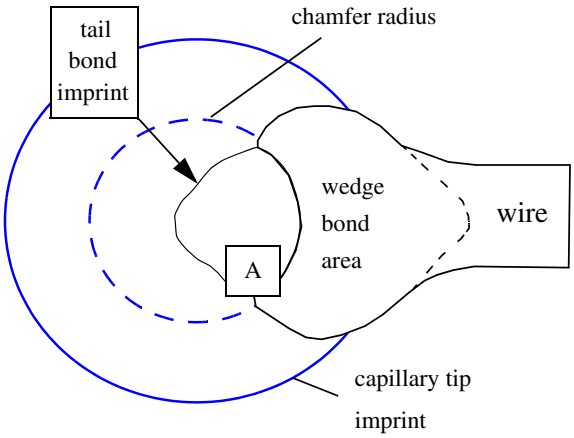

Fig. 1. Top view of illustration of wedge bond.

bonding process is further investigated here using scanning electron microscope (SEM) images of imprints as illustrated in Fig. 1.

3. Experimental

3.1. Materials and equipment

An ESEC WB 3100 wire bonder is used with ball grid array (BGA) substrates that have a Au/Ni (1 μm/5 μm) metallization to which the wires are bonded. Cu and Au wires of 99.99% purity and 25 μm diameter, both available from MK Electron Co. Ltd., Yongin, South Korea, are used for bonding. The capillary used has tip, chamfer and hole diameters of 100 μm, 51 μm, and 35 μm, respectively, and a chamfer angle of 90°.

All free air ball (FAB) samples have diameters of 50 μm and are produced within a period of 30 min using a nominal substrate temperature of 150 °C and a shielding gas mixture of 95% N_2 and 5% H_2. The samples are removed from the bonder, mounted with epoxy at ambient temperature, and cross-sectioned.

3.2. Tail bond process modifications

Three bond-off process modifications are made, serving the respective purposes of providing pick up evidence, understanding the pick up process better, and comparing the FABs produced with and without pick up. Process modification 1 (PM1) is a standard bond-off of the required wire end sample followed by a manual bending operation, as shown in Fig. 2a–d. In Fig. 2a, after creating a wire tail, the wire tail is manually bent using a stiff wire as a tool, as indicated by the arrow in Fig. 2b. In the next step, a standard wedge bond is formed. In Fig. 2c, the standard bond-off process has left the bent wire piece on the metallization. In Fig. 2d, one more bending operation is manually carried out, resulting in the remaining wire standing perpendicular to the substrate and ready for SEM observation. Examples of resulting samples are shown in Fig. 3.

Process modification 2 (PM2) allows to study the flattened zone of the wire that was pressed to the substrate and is illustrated in Fig. 4a–h. In Fig. 4a, after creating a tail, it is carefully bent as shown in Fig. 4b. In Fig. 4c, the ultrasound parameter is set to zero to make a non-bonding bond-off (wedge bond) operation, creating the flattened area on the wire piece which is now accessible. The lack of ultrasound (*US*) results in the wire not sticking on the metallization as shown in Fig. 4d. In Fig. 4e, the wire is bent again, and a normal, successful bond-off is performed with *US*, bonding force (*BF*), and impact force (*IF*) of 60%, 450 mN, and 1000 mN, respectively. Due to the *US* level used, the bent wire piece remains bonded on the metallization Fig. 4f and is then broken Fig. 4g. The remaining wire piece is bent one more time to expose the initial contact area of the wire piece for SEM observation as shown in Fig. 4h.

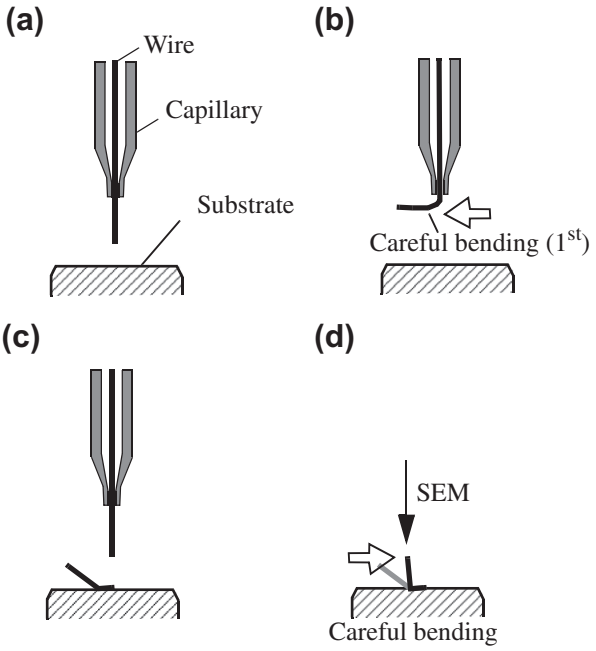

Fig. 2. Illustration of bond-off process modification 1 (pick up).

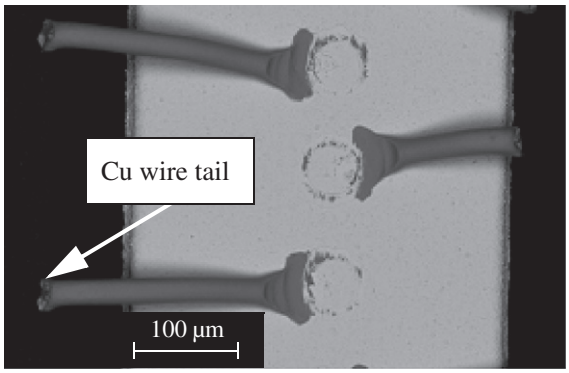

Fig. 3. Bond-off process without prior EFO fire exposing the tail end underside.

Process modification 3 (PM3) aims to obtain FABs without substrate material pick up. The FAB diameters with and without pick up are not different [16]. The bond-off process is modified as illustrated in Fig. 5a–f. In Fig. 5a, a single EFO is carried out to produce a 50 μm diameter FAB. In Fig. 5b, a ball is bonded using the normal bond-off operation without bending the wire. In Fig. 5c, during the subsequent wire breaking operation, the wire breaks in the heat-affected zone above the ball. A tail without any pick up is produced. In Fig. 5d, an EFO is made to the wire material which had no physical contact to the substrate metallization. In Fig. 5e, the resulting FAB will be bent over manually to allow for a normal bond-off. In Fig. 5f, a normal bond-off is made. The FAB sample is fixed to the substrate and ready for inspection.

3.3. Characterization

SEM in backscatter electron (BSE) mode is used to identify and quantify the material remaining on the imprint (bond-off site) after

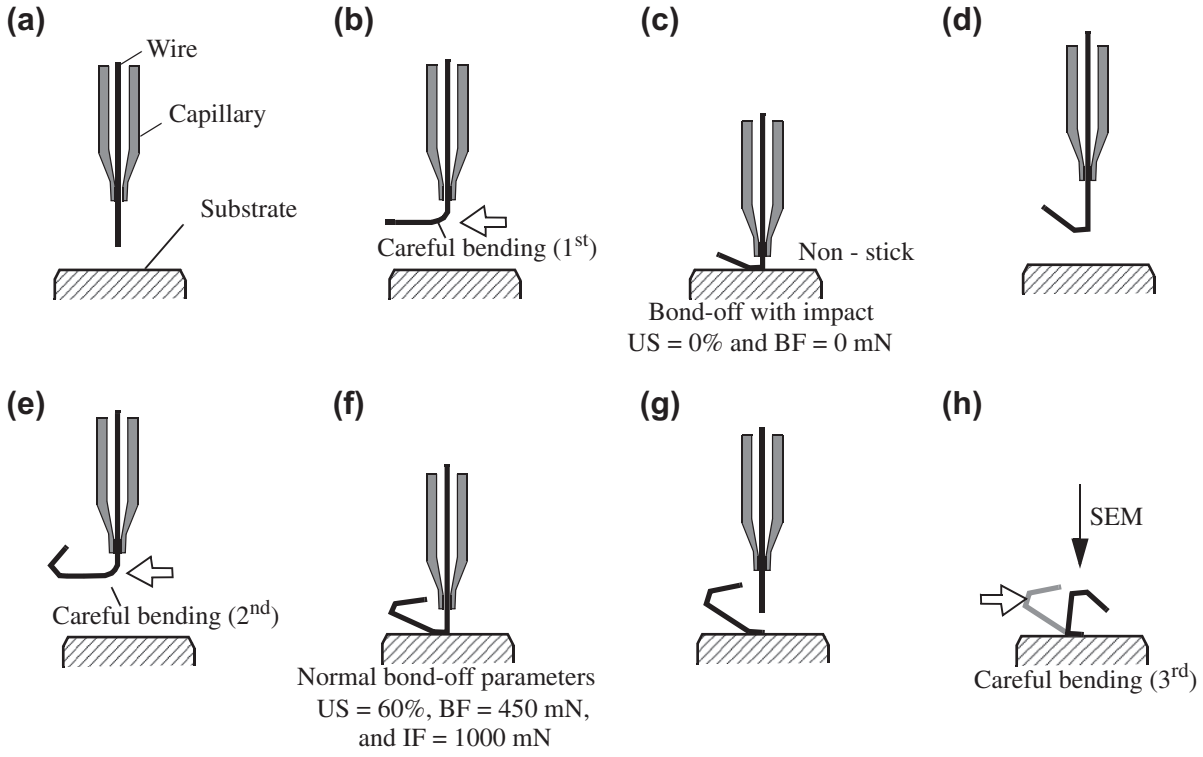

Fig. 4. Illustration of bond-off process modification 2 (pick up without *US*).

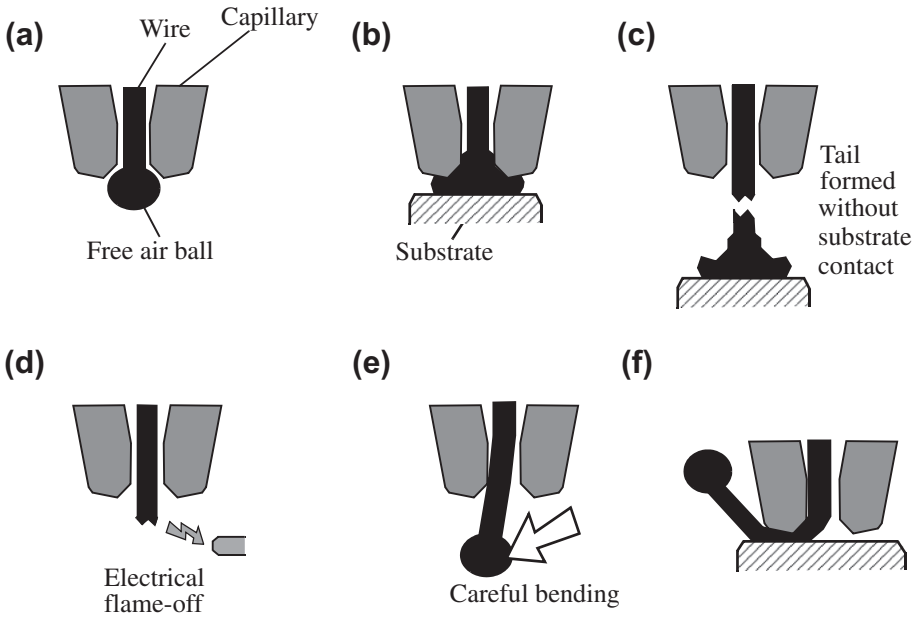

Fig. 5. Illustration of bond-off process modification 3 (FAB without pick up).

tail breaking. Energy dispersive X-ray (EDX) is used to analyze the presence of materials on the tail bond imprint.

A Leco DM-400 Micro-hardness tester is used to make up to three indentations per cross-sectioned FAB. The holding time is 15 s. The Vickers Hardness (HV) is calculated with $HV = 1.854 \times F/D^2$, where $F = 50$ mN is the applied indentation force and D is the area of indentation measured with an optical microscope with image-pro software (Media cybernetics, Bethesda, MD, USA). An example of a cross-sectioned FAB with indentation marks is shown in Fig. 6.

4. Results and discussion

4.1. Pick up of substrate metallization material by wire tail

The SEM image of an imprint area A as defined in Fig. 1 is shown in Fig. 7, showing ductile fractures indicated by α. The BSE image of a similar sample produced with the same process is shown in Fig. 8 and confirms that no Cu residue piece is left on the substrate and that the fracture occurs inside the substrate material. The study of BSE images of wire tails confirms that substrate material is

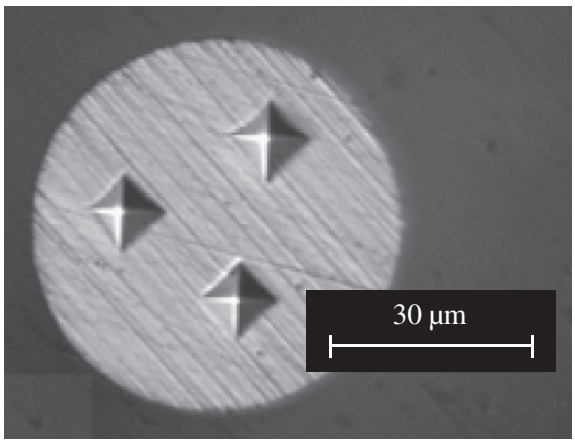

Fig. 6. Optical micrograph of indentation marks.

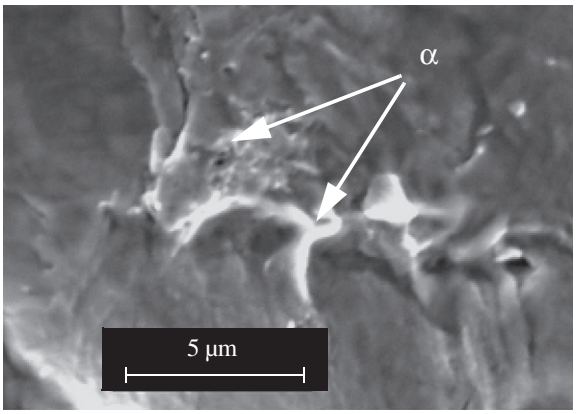

Fig. 7. SEM of Cu tail bond imprint on Au plated substrate showing fractured area of A in Fig. 1a.

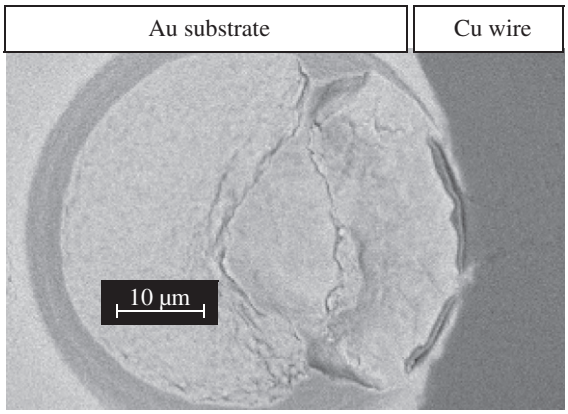

Fig. 8. Tail bond imprint made with Cu wire on Au ball grid array (BGA) substrate.

picked up by the Cu wire as shown by the bright colored residues in Fig. 9. The EDX result shown in Fig. 10 confirms that the white areas in Fig. 9 are Au. *IF*, *US*, *BF*, bonding time (*BT*), and bonding temperature (*T*) are used that equal to 1000 mN, 80%, 500 mN, 25 ms, and 150 °C, respectively. The unit "%" is used for the *US* parameter, and is proportional to the peak to peak vibration amplitude, A_{PP} , measured at the center of the transducer tip: *US* [%] = A_{PP} [nm]/26.6 [nm/%].

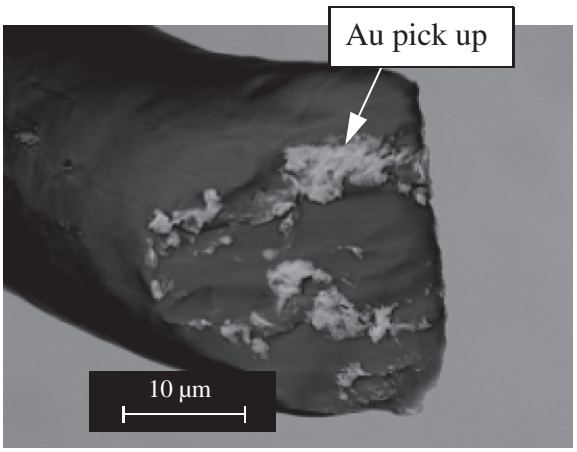

Fig. 9. BSE micrograph of Au pick up found on Cu tail.

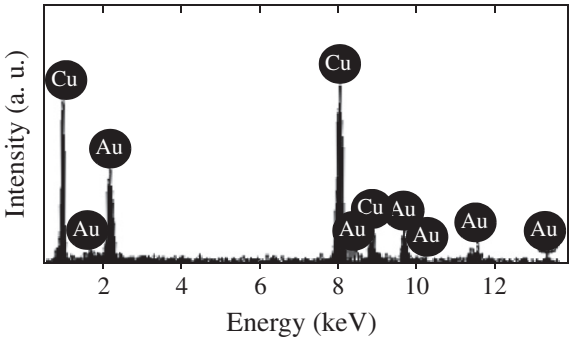

Fig. 10. EDX result of white area indicated by arrow in Fig. 9.

4.2. Influence of process parameters on pick up

Two types of experiments are carried out to study the effects of bonding parameters on the amount of pick up. The first corresponds to a force only process, and the second to an ultrasonic friction process which combines force with ultrasound. The force only process does not result in successful bonding and is studied here only as a reference for the ultrasonic friction process. Ultrasound is a prerequisite for strong bonding quality if the substrate temperature is below 200 °C due to the shear stresses and wear produced at the interface [17].

4.3. Force without ultrasound

Bonds are made without ultrasound to study Au pick up caused by only Cu deformation. The tail bond process used is PM2. The *IF* value is varied from 200 mN to 1200 mN in 200 mN steps while *US*, *BF*, *BT*, and *T* are fixed to 0%, 0 mN, 5 ms, and 150 °C, respectively.

The wire contact area (WCA) is investigated with BSE as shown in Fig. 11a–d which are the samples after application of *IF*s of 200, 600, 800, and 1200 mN, respectively. Au pick up is found on the Cu wire with each tested *IF* value and its size is about 1 μm.

The wire deformation (*WD*), width of WCA, is measured as indicated by arrows and the dashed line across the WCA in Fig. 11a. The value of *WD* produced with *IF* = 200 mN is small. As *IF* is increased to 600 mN, circular substructures are observed on the WCA (Fig. 11b) and illustrated in Fig. 12a. With *IF* = 800 mN, the WCA is elongated toward the wedge bond as indicated by A (Fig. 11c).

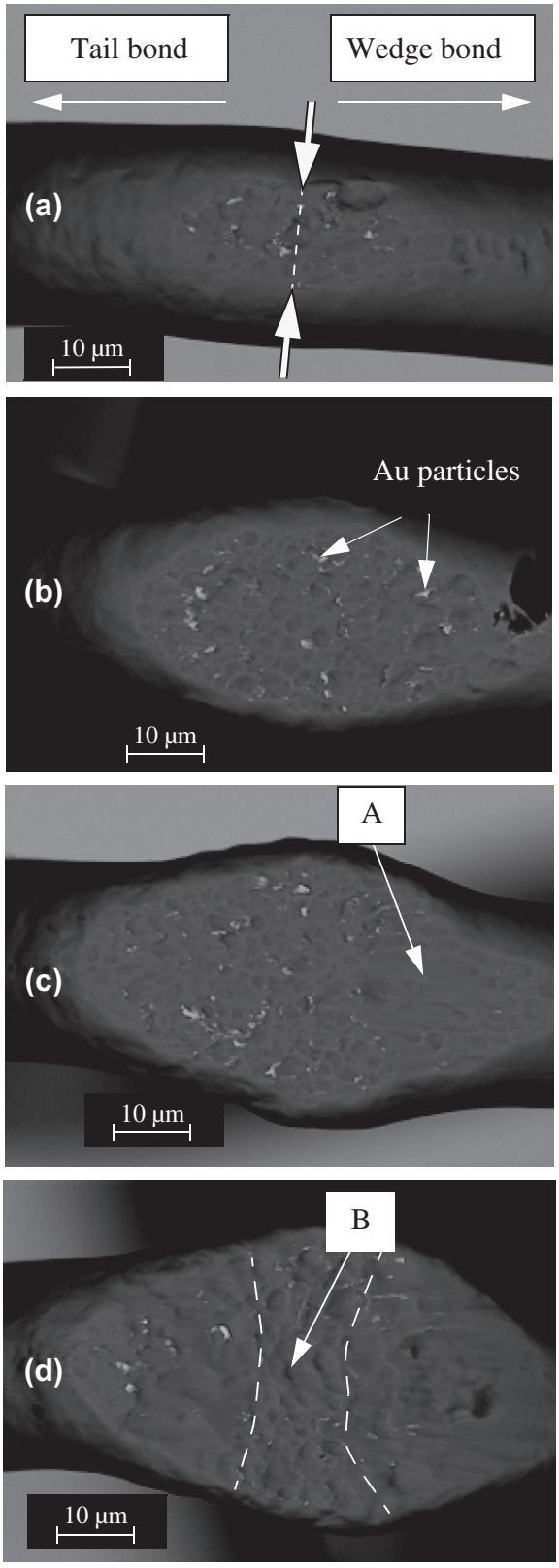

Fig. 11. SEM images of Cu wire contact areas obtained with *IF* of (a) 200 mN, (b) 600 mN, (c) 800 mN, and (d) 1200 mN after been pressed on Au metallization. No ultrasound. Au particles ≈1 μm in size found with all *IF* values.

The substructures have an elongated shape with *IF* of 1200 mN (Fig. 11d) towards both wire directions, while circular substructures remain in the centre as indicated by B. This observation is

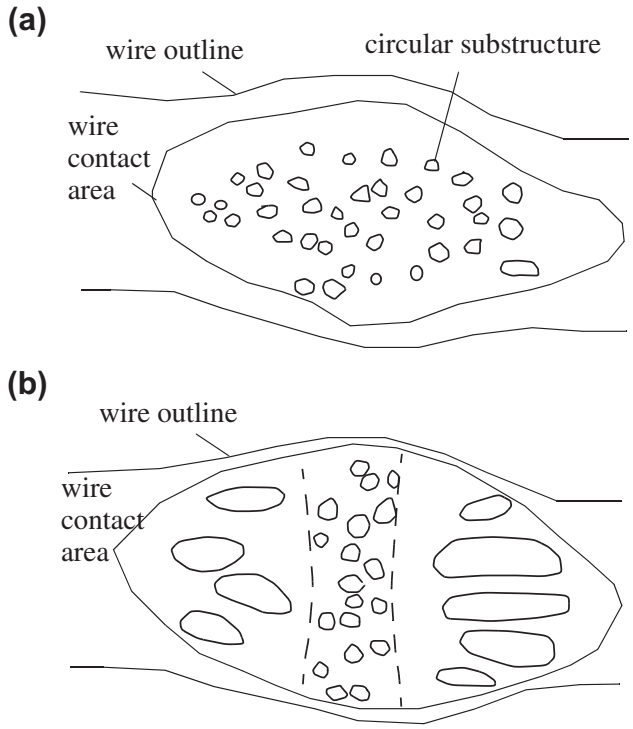

Fig. 12. Illustrations of contact area on Cu wire with *IF* of (a) 600 mN and (b) 1200 mN. No ultrasound.

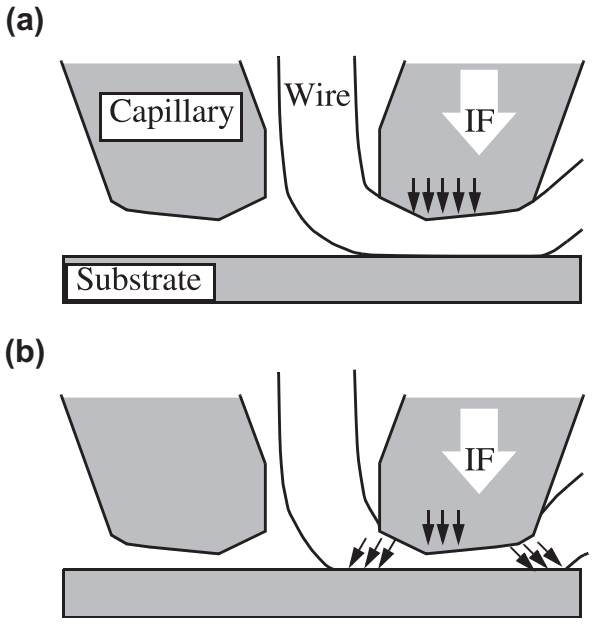

Fig. 13. Illustrations of normal and shear force applied during impact. (a) Low *IF* and (b) high *IF*.

illustrated in Fig. 12b and discussed using the illustrations in Fig. 13a and b. With low *IF*, Cu wire deformation occurs mainly along the *IF* direction (normal force) as shown in Fig. 13a. As *IF* increases, the wire is further deformed and pushed to the wire directions creating a lateral material flow component as illustrated in Fig. 13b, amplified by the angles between capillary tip surface and substrate. This material flow causes the elongated shapes of the imprint structures.

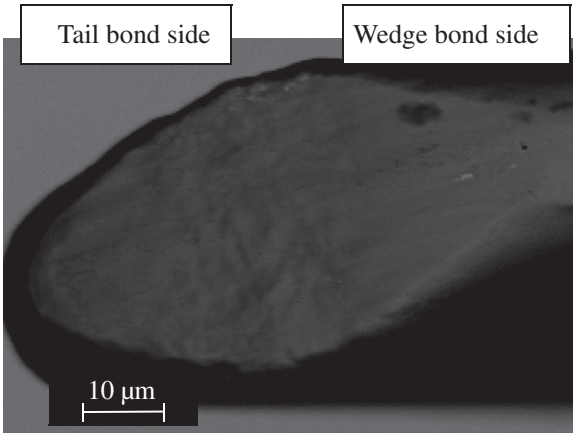

Fig. 14. SEM of imprint of Cu wire made on Ag leadframes with *IF* of 800 mN.

In contrast to Au metallization, material pick up is not observed on the Cu tail if Ag metallization (Fig. 14) and the following bonding parameters are used: *US* = 0%, *IF* = 800 mN, *BF* = 0 mN, *BT* = 5 ms, and *T* = 220 °C. The thickness of the Ag metallization is 8 µm.

4.4. Ultrasound with force

To obtain a stable tail breaking force (TBF), the *BF* is recommended to be under tight control [18], e.g. by fixing it to *BF* = 450 mN, while *US* and *IF* are varied for the following study. Other bonding parameters are *BT* = 25 ms and *T* = 150 °C. PM1 is further used to quantify the amount of Au pick up with various *US* parameters. The bonding parameters selected are all combinations of *IF* = [400, 700, 100] mN with *US* = [0, 50, 55, 60, 65, 70]%.

The area covered by Au pick up material is quantified with the analysis software of the SEM (JEOL, Tokyo, Japan). Fig. 15 shows the measured area of Au pick up, revealing the strong effect of *IF*. Each value given is the average of 10 samples. The errorbars represent $\varepsilon = \sigma/(\sqrt{n-1})$ where σ is the standard deviation and n is the number of measurements.

As *IF* is increased, the area of Au pick up decreases. With *IF* = 400 mN, the Au pick up area increases ≈30% as *US* is increased from 50% to 60% and then tends to fluctuate for *US* between 60% and 70%. With *IF* higher than 700 mN, no influence of *US* on Au pick is observed. Fig. 16a and b are example SEM images showing pick up obtained with *IF* of 400 mN and 1000 mN, respectively. *US*, *BF*, *BT*, and *T* are 60%, 450 mN, 25 mN, and 150 °C, respectively.

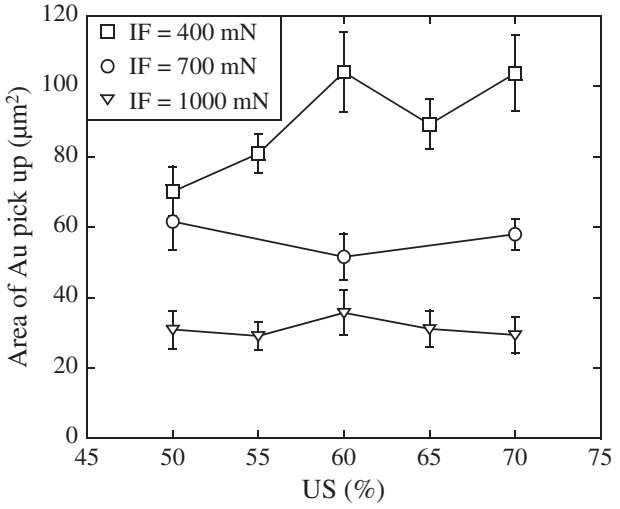

Fig. 15. Au pick up changes with various *US* and *IF*.

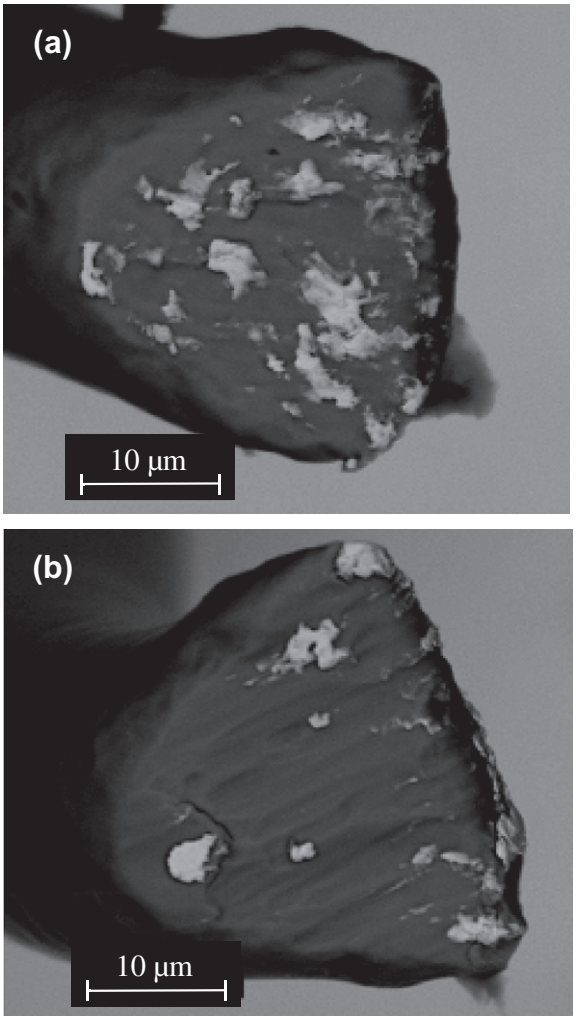

Fig. 16. Au pick ups with *IF*s of (a) 400 mN and (b) 1000 mN.

The relatively high amount of Au pick up observed with *IF* = 400 mN may be due to the type of deformation the wire experiences. The total *WD* is the sum of impact type deformation (*ID*), and ultrasound enhanced deformation (UED), *WD* = *ID* + UED. During UED, ultrasonic friction occurs at the interface as the wire deforms. The friction forces not only produce additional interfacial wear, but also additional stress in the wire, allowing to achieve larger plastic deformation with less force.

An example measurement is shown in Fig. 17 for which bonding parameters used are *IF*, *US*, *BF*, *BT*, and *T* of 800 mN, 0%, 0 mN, 5 ms,

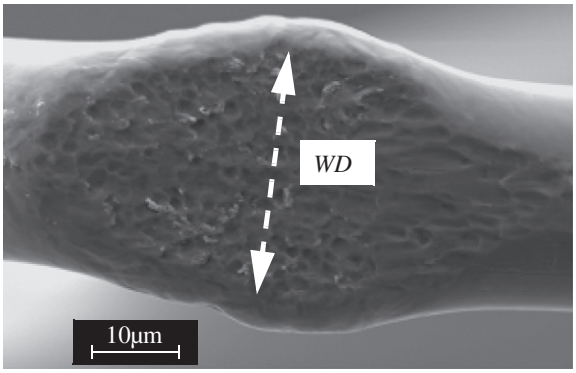

Fig. 17. SEM image showing an example measurement of the wire deformation.

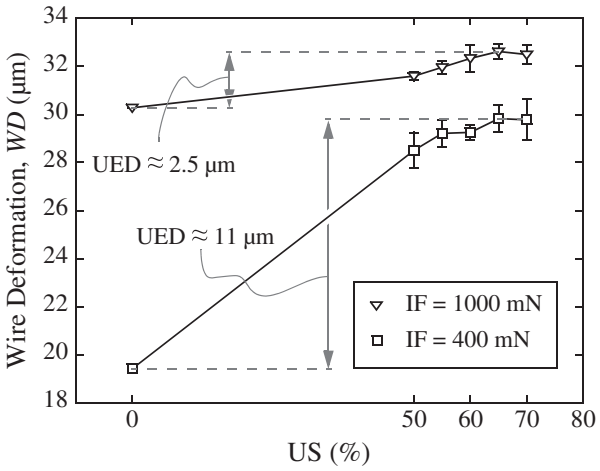

Fig. 18. Increase of tail bond deformation with *US* and *IF*.

and 150 °C. Fig. 18 shows experimental results of the *WD* obtained with various *US* values between 0% and 70% and a low and a high *IF* value. With the higher *IF* = 1000 mN, *ID* is 30 μm and UED adds only 2.5 μm more with *US* = 70%. In contrast, with the lower *IF* = 400 mN, *ID* is about 19 μm and UED adds 11 μm (>50%) more with *US* = 70%. For such relatively low *IF* values, ultrasound plays a dominant role in wire deformation. Compared to *ID*, UED is assumed to produce more interfacial wear due to the *US* present in the process. Therefore, it can be concluded that UED can play an important role in Au pick up.

4.5. Effect of Au pick up on FAB hardness

The two *IF* values 400 mN and 1000 mN are selected to produce Cu FABs with higher and lower amounts of Au pick up, respectively. FABs without pick up are produced with PM3 and used for reference. The FAB hardness results are shown in Fig. 19. The average hardness decreases as the amount of Au pick up is increased. The FAB hardness average and standard deviation values measured for zero, low, and high amounts of pick up are 76.8 ± 3.4 HV, 75.5 ± 7.14 HV, and 74 ± 6.0 HV, respectively. The *t*-test results of the micro-hardness are summarized in Table 1. It indicates that the hardness of FAB is significantly (95% confidence level) reduced by the Au pick up if *IF* = 400 mN. The standard deviations with Au

Table 1
FAB micro-hardness compared to zero pick up FABs: *t*-values for FABs obtained after bond-off with *IF* of 400 and 1000 mN. The sample size is 30.

IF (mN)	*t*-value	Significant difference
400	2.20	Yes
1000	0.91	No

pick up are significantly larger than that without pick up. This might be due to the relatively large variation of the Au pick up amounts observed for a given set of bonding parameters. The distribution shape of Au in the FAB is not known. Impurities might accumulate on the ball surface during melting and solidification. In such a case, hardness measurements on FAB cross sections would not be sensitive to impurities. However, when investigating the surface of FAB before cross-sectioning with EDX, no Au was obvious on the surface. In this investigation, an uniform distribution of Au is assumed. For future research, finding how Au is distributed in the FAB would be an interesting topic.

In theory, Cu hardens upon addition of Au as a dopant [19]. However, standard Cu bonding wire already has a variety of dopant elements with hardening effects. The additional Au can interfere with the previously present dopant elements during melting and solidification in the EFO process, possibly resulting in less hardening. A small amount of dopant addition in Cu wire can change the FAB hardness [20]. This would appear as the bit of softening observed here compared to the case without Au pick up.

It is known that the higher hardness of Cu balls compared to that of Au balls may cause chip damage [6,8,11,21]. Onuki [11] reported that with decreasing ball hardness, chip damage decreases and disappears when the hardness of the ball decreases to a certain value. Hence, hardness values can be used for upper specification limit (USL) for chip cratering.

Using the hardness data of Fig. 19, values of process capability index (*cpk*) are calculated for each set of results using $cpk = (\mathrm{USL} - \overline{H_H V})/3\sigma$ where $\overline{H_H V}$ is the average hardness.

To visualize the effect of the standard deviation on process capability, *cpk* values with various values for USL are shown in Fig. 20. For $cpk_{\mathrm{HV}} > 2$, a USL higher than 119 HV and 110 HV for *IF* = 1000 mN and *IF* = 400 mN, respectively, is sufficient. Assuming that chip damage occurs as soon as the FAB hardness is above USL, it can be concluded that in spite of reducing the average FAB hardness, substrate material pick up by the Cu wire tail increases the probability of chip damage. This is due to the larger FAB hardness standard deviation.

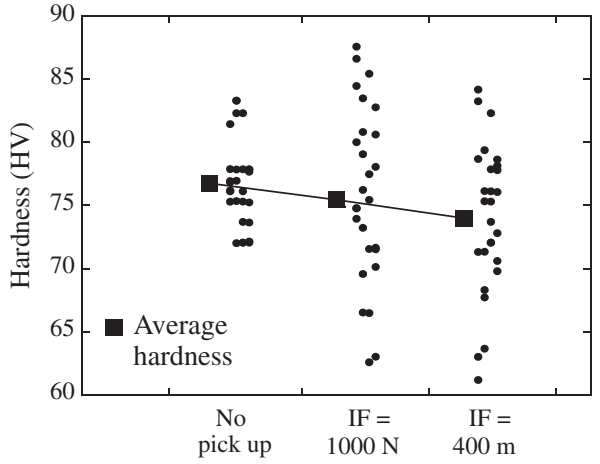

Fig. 19. Hardness comparison of Cu FABs with various amounts of Au pick up (sample size 30).

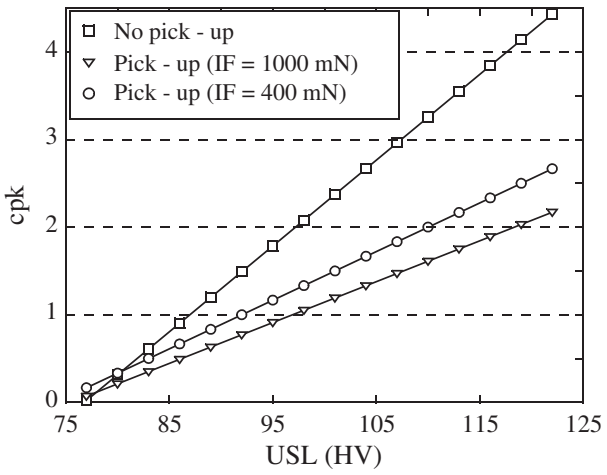

Fig. 20. Cpk values calculated from data in Fig. 19 as USL is increased.

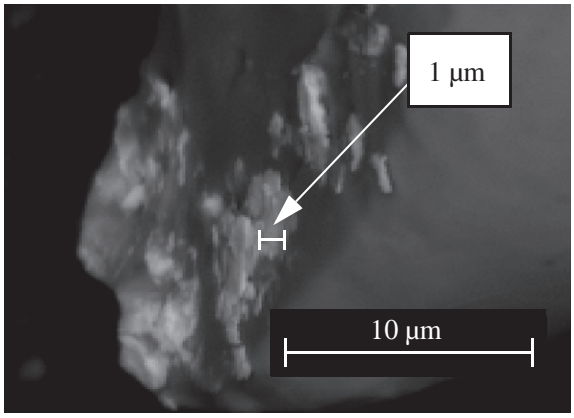

Fig. 21. Thickness of Au pick up. Thickness of Au pick up ranges between 0.1 μm and 1.0 μm. Average thickness of Au pick up estimated to be 0.5 μm.

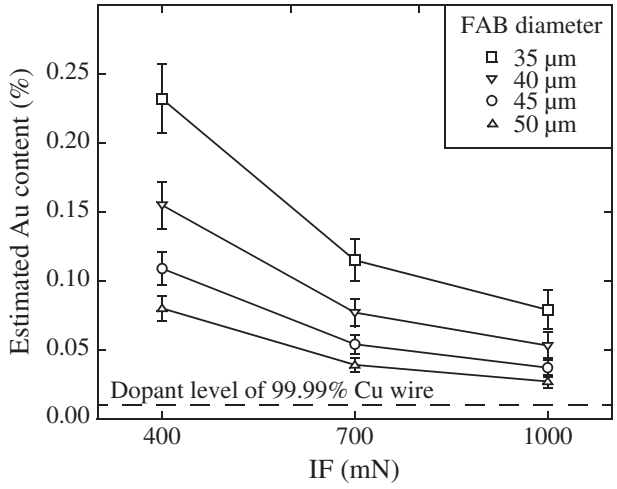

Fig. 22. Estimated Au pick up content in Cu FAB after bond-off with various *IF* and for various FAB diameters.

4.6. Pick up volume estimation

The estimated volumetric fractions of Au in the 50 μm diameter Cu FABs obtained with *IF* = 400 mN and *IF* = 1000 mN, assuming an average pick up thickness = 0.5 μm as derived from Fig. 21, are 0.08% and 0.03%, respectively. As the wire used is rated 99.99% pure Cu, it contains less than 0.01% (100 ppm) impurities. The estimated Au contents from pick up exceeds this specified impurity content. The relative Au content increases as the FAB diameter decreases as extrapolated in Fig. 22. For a FAB that is 35 μm in diameter, the Au content can be 0.23% according to this extrapolation.

5. Conclusions

1. The Cu wire tail always picks up Au from the substrate during the tail breaking process.
2. The lower the impact force, the more ultrasound enhanced deformation dominates over impact deformation, enhances the interfacial wear during bonding, and increasing the amount of Au pick up on the Cu tail.
3. The amount of Au pick up estimated in the Cu FAB exceeds the typical impurity and dopant levels in the wire.
4. Compared with FABs obtained without pick up, FABs with Au pick up have a lower average FAB hardness, but a wider standard deviation. Therefore, Au pick up in Cu FAB can lead to more FABs that are exceptionally hard and subsequently to more chip damage.

Acknowledgements

This work is supported by MK Electron Co. Ltd. (Yongin, Korea), Microbonds Inc. (Markham, Canada), NSERC, AuTEK, and OCE (all from Canada).

References

[1] Assembly and packaging. International technology roadmap for semiconductors, ITRS update; 2006. p. 1–19.
[2] Onuki J, Koizumi M, Araki I. Investigation of the reliability of copper ball bonds to aluminum electrodes. IEEE Trans Comp Hybrids Manuf Technol CHMT-12 1987:550–5.
[3] Aoh JN, Chuang CL. Development of a thermosonic wire bonding process for gold wire bonding to copper pads using argon shielding. J Electron Mater 2004;33:300–11.
[4] Beleran J, Turiano A, Calpito DM, Stephan D, Saraswati, Wulff F, et al. Tail pull strength of Cu wire on gold and silver-plated bonding leads. Proc SEMICON 2005:1–8.
[5] Winchell VH, Berg HM. Enhancing ultrasonic bond development. IEEE Trans Comp Hybrids Manuf Technol CHMT-1 1978:211–9.
[6] Toyozawa K, Fujita K, Minamide S, Maeda T. Development of copper wire bonding application technology. In: Proc Electron Comp Conf, Las Vegas, NV, USA, 1990. p. 762–7.
[7] Tummala R, Rymaszewski E, Klopfenstein A. Microelectronics packaging handbook – part 2. Massachusetts (USA): Kluwer Academic Publishers; 1997. p. 481–2.
[8] Harman G. Wire bonding in microelectronics materials, processes, reliability, and yield. 2nd ed. New York: McGraw-Hill; 1997. p. 203–7.
[9] Koyama H, Shiozaki H, Okumura I, Mizugashira S, Higuchi H, Ajiki T. A new bond failure wire crater in surface mount device. In: Ann proc reliab phys symp, Montrey, California, USA, 1988. p. 59–63.
[10] Deley M, Levine L. Copper ball bonding advances for leading edge packaging. Singapore: SEMICON; 2005. pp. 1–4.
[11] Onuki J, Koizumi M, Suzuki H, Araki I, Iizuka T. Influence of ball-forming conditions on the hardness of copper balls. J Appl Phys 1990;68:5610–4.
[12] Wei TC, Daud AR. Cratering on thermosonic copper wire ball bonding. J Mater Eng Perform 2002;11:283–7.
[13] Tan J, Zhong ZW, Ho HM. Wire-bonding process development for low-*k* materials. Microelectron Eng 2005;81:75–82.
[14] Zhang L, Grmaste V, Poddar A, Nguyen L, Schulze G. Analytical and experimental characterization of bonding over active circuitry. J Electron Packag 2007;129:391–9.
[15] Lee J, Mayer M, Zhou Y, Hong SJ. Iterative optimization of tail breaking force of 1mil wire thermosonic ball bonding processes and the influence of plasma cleaning. Microelectron J 2007;38:842–7.
[16] Lee J, Mayer M, Zhou Y, Hong SJ, Moon JT. Silver pick-up during tail formation and its effect on free air ball in thermosonic copper ball bonding. In: Electron comp technol conf USA, 2008. p. 2024–9.
[17] Zhou Y, Li X, Noolu NJ. A footprint study of bond initiation in gold wire crescent bonding. IEEE Trans Comp Packag Technol 2005;28:810–6.
[18] Lee J, Mayer M, Zhou Y, Hong SJ, Moon JT. Concurrent optimization of crescent bond pull force and tail breaking force in a thermosonic Cu wire bonding process. IEEE Trans Electron Packag Manuf 2009;32:157–63.
[19] Lin DS, Wilman H. Friction, wear and surface hardness in abrasion of binary solid-solution alloys in the copper–gold system. Br J Appl Phys 1968;1:561–72.
[20] Hang CJ, Lim I, Lee J, Mayer M, Wang CQ, Zhou Y, et al. Bonding wire characterization using automatic deformability measurement. Microelectron Eng 2008;85:1795–803.
[21] Nguyen L, Mcdonald D, Danker A, Ng P. Optimization of copper wire bonding on Al–Cu metallization. IEEE Trans Comp Packag Manuf Technol Part A 1995;18:423–9.